Int. J. Electrochem. Sci., 6 **(2011)** 691 - 704

International Journal of
ELECTROCHEMICAL
SCIENCE
www.electrochemsci.org

Chemical Composition and Inhibitory Effect of *Mentha Spicata* Essential Oil on the Corrosion of Steel in Molar Hydrochloric Acid

M. Znini[1], *M. Bouklah*[2], *L. Majidi*[1,*], *S. Kharchouf*[1], *A. Aouniti*[2], *A. Bouyanzer*[2], *B. Hammouti*[2], *J. Costa*[3], *S.S. Al-Deyab*[4]

[1] Laboratoire des Substances Naturelles & Synthèse et Dynamique Moléculaire, Faculté des Sciences et Techniques, Université Moulay Islmail, Errachidia, Morocco.
[2] LCAE-URAC18, Faculté des Sciences, Université Mohammed Premier, BP 4808, Oujda, Morocco.
[3] Université de Corse, UMR CNRS 6134, Laboratoire de Chimie des Produits Naturels, Faculté des Sciences et Techniques, Corse, France.
[4] Department of Chemistry, College of Science, King Saud University, B.O. 2455, Riaydh 11451, Saudi Arabia.
[*]E-mail: lmajidi@yahoo.fr

Received: 4 October 2010 / *Accepted:* 20 January 2011 / *Published:* 1 March 2011

The essential oil from aerial parts of *Mentha spicata* L. an aromatic member of the Lamiaceae family, collected from "Tazouka" (Errachidia-Morocco), was obtained by hydrodistillation using Clevenger apparatus and analyzed by GC and GC/MS. The constituents were identified by their Mass spectra and Retention indices. Forty one compounds consisting 91.90% of the total components were identified from the oil obtained. Among those, Carvone (29.00%) and Trans carveol (14.00%) were the major oil components. The inhibitory effect of this oil was estimated on the corrosion of steel in 1M hydrochloric acid using electrochemical polarisation and weight loss measurements. The corrosion rate of steel is decreased in the presence of natural oil. The inhibition efficiency was found to increase with oil content to attain 97% at 2.00 g/l. Polarisation curves revealed that this natural oil act as mixed type inhibitor. The temperature effect on the corrosion behaviour of steel in 1M HCl without and with the inhibitor at 2.00 g/l was studied in the temperature range from 303and 333 K, the associated activation energy have been determined. The adsorption of oil on the steel surface was found to obey Langmuir's adsorption isotherm. EIS measurements show that the increase of the transfer resistance with the inhibitor concentration.

Keywords: Corrosion inhibition, steel, *Mentha spicata* L., Essential oil, adsorption. hydrodistillation

1. INTRODUCTION

Efforts to stop or delay to the maximum the attack of metals in various corrosive media are made. Nevertheless, the known hazard effects of the most synthetic inhibitors and the need to develop

on the use of natural products. Near their environmental and acceptable ecolological properties, naturally occurring antioxidants are cheap and readily available and renewable sources of materials [1-4]. These organic compounds are either synthesized or either extracted from aromatic herbs, spices and medicinal plants. These advantages have incited us to draw a large part of program of our laboratory to examine extracts of natural substances as corrosion inhibitors. We previously reported that Pennyroyal oil [5], Eucalyptus oil [6], Fenugreek oil [7], menthol derivatives [8], *Artemisia herba alba* oil [9], have been found to be very efficient corrosion inhibitors for steel in acid media. In this paper, our choice is focused to essential oil of spearmint (*Mentha spicata).* We noted that Mint is the common name of approximately 25 perennial species of the genus Mentha belonging to the *Lamiaceae* family [10]. It is one of the most important herbs traditionally produced in Morrocco. The existence of differences chemotypes, based on qualitative differences within a taxon, is a common feature in most *Mentha* species and hybrids [11]. As a result, the mint plants produce a number of commercially valuable essential oils. Its concentration in the oil varies considerably depending on its genetic and geographical origin.

Mentha spicata L. (spearmint) is a creeping rhizomatous, glabrous and perennial herb with a strong aromatic odor. The oil of *M. spicata* is rich in carvone and presents a characteristic spearmint odor [12]. The fresh and dried plants and their essential oils are widely used in food, cosmetic, confectionary, chewing gum, toothpaste and pharmaceutical industries [13]. A spearmint type grown in Errachidia oasis is highly valued for its distinguished aroma. It is locally known as "Tazouka mint".The present study was aimed to extraction, characterization and test by electrochemical measurements and gravimetric methods, the effect of *Mentha spicata* oil of Errachidia region on the corrosion of steel in 1M HCl solution. Effect of temperature is also studied.

2. EXPERIMENTAL PART

2.1. Extraction of Mentha essential oil

The aerial part of *Mentha spicata* was harvested in May 2007 in Tazouka (Errachidia) located at the south-east of Morocco. The dried plant material is stored in the laboratory at room temperature (298 K) and in the shade before the extraction. The extraction of essential oil of the aerial part of *M. spicata* was conducted by hydrodistillation using a Clevenger type apparatus [14], and the essential oil yield was 0.53%. The essential oil obtained was dried under anhydrous sodium sulfate and stored at 4 °C in the dark before analysis

2.2. GC analysis

GC analyses were performed using a Perkin Elmer Autosystem GC apparatus (Walhton, MA, USA) equipped with a single injector and two flame ionization detectors (FID). The apparatus was used for simultaneous sampling to two fused-silica capillary columns (60 m x 0.22 mm, film thickness 0.25 lm) with different stationary phases: Rtx-1 (polydimethylsiloxane) and Rtx-Wax (polyethylene

glycol). Temperature program: 60 to 230 °C at 2 °C /min and then held isothermal 230 °C (30 min). Carrier gas: helium (1 $mL.min^{-1}$). Injector and detector temperatures were held at 280 °C. Split injection was conducted with a ratio split of 1:80. Injected volume: 0.1 µL

2.3. Gas Chromatography-mass spectrometry

The oils obtained were investigated using a Perkin Elmer TurboMass Quadrupole Detector, directly coupled to a Perkin Elmer Autosystem XL equipped with two fused-silica capillary columns (60 m x 0.22 mm, film thickness 0.25 µm), Rtx-1 (polydimethylsiloxane) and Rtx-Wax (polyethylene glycol). Other GC conditions were the same as described above. Ion source temperature: 150 °C; energy ionization: 70 eV; electron ionization mass spectra were acquired with a mass range of 35–350 Da. Oil injected volume: 0.1 µL.

2.4. Components identification

Identification of the components was based:

(I) on the comparison of their GC retention indices (RI) on non polar and polar columns, determined relative to the retention time of a series of n-alkanes with linear interpolation, with those of authentic compounds or literature data; [15,16] and

(II) on computer matching with commercial mass spectral libraries [16,17] and comparison of spectra with those of our personal library. Relative amounts of individual components were calculated on the basis of their GC peak areas on the two capillary Rtx-1 and Rtx-Wax columns, without FID response factor correction.

2.5. Measurements

2.5.1. Weight loss tests

The aggressive solution (1M HCl) was prepared by dilution of Analytical Grade 37 % HCl with double-distilled water. Prior to all measurements, the steel samples (0.09% P; 0.38% Si; 0.01% Al; 0.05% Mn; 0.21% C; 0.05% S and the remainder iron) were polished with different emery paper up to 1200 grade, washed thoroughly with double-distilled water, degreased with AR grade ethanol, acetone and drying at room temperature.

Gravimetric measurements were carried out in a double walled glass cell equipped with a thermostat-cooling condenser. The solution volume was 100 ml. The steel specimens used had a rectangular form (2 cm x 2 cm x 0.05 cm). The immersion time for the weight loss was 6 h at 298 ± 1 K. After the corrosion test, the specimens of steel were carefully washed in double-distilled water, dried and then weighed. The rinse removed loose segments of the film of the corroded samples. Duplicate experiments were performed in each case and the mean value of the weight loss is reported. Weight loss allowed us to calculate the mean corrosion rate as expressed in $mg.cm^{-2}\ h^{-1}$.

2.5.2. Rp, polarisation and EIS measurements

Electrochemical measurements were carried out in a conventional three-electrode electrolysis cylindrical Pyrex glass cell. The working electrode (WE) in the form of disc cut from steel has a geometric area of 1 cm^2 and is embedded in polytetrafluoroethylene (PTFE). A saturated calomel electrode (SCE) and a disc platinum electrode were used respectively as reference and auxiliary electrodes, respectively. The temperature was thermostatically controlled at 298 ± 1 K. The WE was abraded with silicon carbide paper (grade P1200), degreased with AR grade ethanol and acetone, and rinsed with double-distilled water before use.

Running on an IBM compatible personal computer, the 352 Soft Corr™ III Software communicates with EG&G Instruments potentiostat–galvanostat model 263A at a scan rate of 0.5 mV/sec. Before recording the cathodic polarisation curves, the steel electrode is polarised at -800 mV for 10 min. For anodic curves, the potential of the electrode is swept from its corrosion potential after 30 min at free corrosion potential, to more positive values. The test solution is deaerated with pure nitrogen. Gas bubbling is maintained through the experiments.

Near E_{corr}, a scan through a potential range performs polarisation resistance measurements. The potential range is ±10mV around E_{corr}. The resulting current is plotted versus potential. Polarisation resistance (R_p) values are obtained from the current potential plot. The scan rate was 0.05 mV/sec.

The electrochemical impedance spectroscopy (EIS) measurements were carried out with the electrochemical system which included a digital potentiostat model Volta lab PGZ 100 computer at E_{corr} after immersion in solution without bubbling, the circular surface of steel exposing of 1 cm^2 to the solution were used as working electrode. After the determination of steady-state current at a given potential, sine wave voltage (10 mV) peak to peak, at frequencies between 100 kHz and 10 mHz were superimposed on the rest potential. Computer programs automatically controlled the measurements performed at rest potentials after 30 min of exposure. The impedance diagrams are given in the Nyquist representation. Values of R_t and C_{dl} were obtained from Nyquist plots.

3. RESULTS AND DISCUSSION

3.1. Mentha spicata essential oil analysis

The analysis of Mentha spicata essential oil allowed the identification of forty one components, which accounted for 91.90% in the total of oil. Their Retention indices (RIs) and their relative percentages are reported in Table 1.

Analyzed essential oil of M. spicata mainly consisted of oxygenated monoterpenes (65.80%) followed by sesquiterpenes hydrocarbons (12.40%), monoterpenes hydrocarbones (9.70), oxygenated sesquiterpenes (2.80%) and oxygenated diterpenes (1.20%). This oil was characterized by the high percentage of C6-oxygenated p-menthane compounds including carvone (29.00%) and trans carveol (14.00%) are major constituents.

Table 1. Chemical composition of *Mentha spicata* essential oil.

N	Components	RI *l*	RI *a*	RI *p*	%
1	Oct-1-en-3-ol	962	961	1395	0.20
2	Sabinene	973	966	1098	0.10
3	β-Pinene	978	971	1085	0.30
4	Octan-3-ol	962	980	1343	2.60
5	Myrcene	987	980	1131	
6	1.8-Cineol	1024	1019	1183	7.30
7	Limonene	1025	1019	1169	
8	Ocimene-β-Z	1029	1022	1202	0.40
9	Ocimene-β-E	1041	1033	1215	0.10
10	Nonanal	1076	1076	1343	0.30
11	Linalool	1086	1078	1493	0.40
12	1-Oct-3-enyl acetate	1093	1087	1329	0.50
13	Octan-3-ol acetate	1123	1102	1294	1.10
14	Camphre	1123	1116	1457	1.00
15	Borneol	1150	1145	1641	0.20
16	Carvone-dihydro-E	1172	1167	1550	0.50
17	dihydro-Carveol	1176	1174	1669	4.50
18	trans-Carveol	1200	1199	1775	14.00
19	Carvone	1214	1218	1675	29.00
20	Bornyl acetate	1270	1267	1527	0.20
21	Dihydroedulan	1290(DB5)	1279	1469	0.80
22	Dihydroedulan	1290(DB5)	1283	1443	3.20
23	Carvacrol	1278	1283	2129	
24	Carvyl-dihydro-acetate-iso	-	1288	1580	0.60
25	Carvyl-dihydro-acetate-neoiso	-	1309	1616	0.70
26	Carvyl-acetate-Z	1318	1317	1679	6.70
27	Carvyl-acetate-E	1345	1343	1711	0.60
28	Jasmone-E	1356	1368	1876	0.20
29	β-Bourbonene	1386	1384	1475	2.90
30	trans-Caryophyllene	1421	1419	1550	3.20
31	Farnesene-E-β	1446	1450	1621	0.60
32	α-Humulene	1455	1452	1616	0.50
33	Germacrene-D	1479	1479	1647	3.90
34	Bicyclogermacrene	1494	1494	1679	0.90
35	δ-Cadinene	1520	1519	1692	0.40
36	Caryophyllene oxide	1578	1573	1917	0.90
37	epi-Cubenol	1623	1608	1990	0.20
38	Caryophylla-4(14).8(15)dien-5α-ol	1641 PETU	1623	2215	1.00
39	τ-Cadinol	1633	1632	2098	0.30
40	α-Cadinol	1643	1644	2158	0.40
41	Phytol-E	2114	2111	2549	1.20

Table 1. Continued	
Total identified	91.90
Monoterpene Hydrocarbons	9.70
Sesquiterpene Hydrocarbons	12.40
Oxygenated Monoterpenes	65.80
Oxygenated Sesquiterpenes	2.80
Oxygenated Diterpene	1.20

Order of elution are given on apolar column (Rtx-1)

RI *l* = retention indices on the apolar column of literature

RI *a* = retention indices on the apolar column (Rtx-1)

RI *p* = retention indices on the polar column (Rtx-Wax)

% = relative percentages of components are given on the apolar column.

The data presented here are in agreement with those reported in previous studies [11,18,19]. The variations in oil content and oil composition could, apparently, be attributed to factors related to ecotype, phenophases and the environment including temperature, relative humidity, irradiance and photoperiod [20].

3.2. Weight loss tests

The corrosion rate (W_{corr}) of steel in 1M HCl solution at various contents of the natural oil tested was determined after 6 h of immersion period at 298 ± 1 K. Values of corrosion rates and inhibition efficiencies are given in Table 1. In the case of the weight loss method, the inhibition efficiency (E_w %) was determined by the following relation:

$$E_w\,\% = \frac{W_{corr} - W_{corr\,(inh)}}{W_{corr}} \times 100 \qquad (1)$$

where W_{corr} and $W_{corr\ (inh)}$ are the corrosion rates of steel in the absence and presence of the oil, respectively.

The analysis of these results (Table 2 and Fig. 1) shows clearly that the corrosion rate decreases (W ($mg/h.cm^2$) while the inhibition efficiency (Ew (%)) increases with increasing inhibitor concentration reaching a maximum value of 97% at a concentration of 2.00 g/l. This behavior can be attributed to the increase of the surface covered θ (Ew %/100) and that due to the adsorption of natural compounds on the surface of the metal as the inhibitor concentration increases. We can conclude that Mentha oil is a good corrosion inhibitor for steel in 1M HCl solution.

3.3. Polarisation measurements

Current-potential characteristics resulting from cathodic polarisation curves of steel in molar HCl at various concentrations of the tested of Mentha oil is evaluated. Fig. 2 shows the typical cathodic Tafel plots of the Mentha oil at different concentrations.

Table 3 collects the corrosion kinetic parameters such as E_{corr}, I_{corr} and β_c obtained from potentiodynamic polarization curves for steel in 1M HCl containing different concentrations of Mentha oil. In the case of polarization method the relation determines the inhibition efficiency (E_I %):

Table 2. Gravimetric results of steel in acid without and with addition of the natural oil at various contents (*t*= 6h. *T*= 298 ± 1 K).

Concentration (g/l)	W (mg/cm^2 .h)	E(%)
blanc	0.3810	
0.125	0.1879	51
0.250	0.1220	68
0.345	0.1194	69
0.500	0.0910	76
0.625	0.0880	77
0.75	0.0800	79
1.00	0.051	87
1.50	0.023	94
2.00	0.015	97

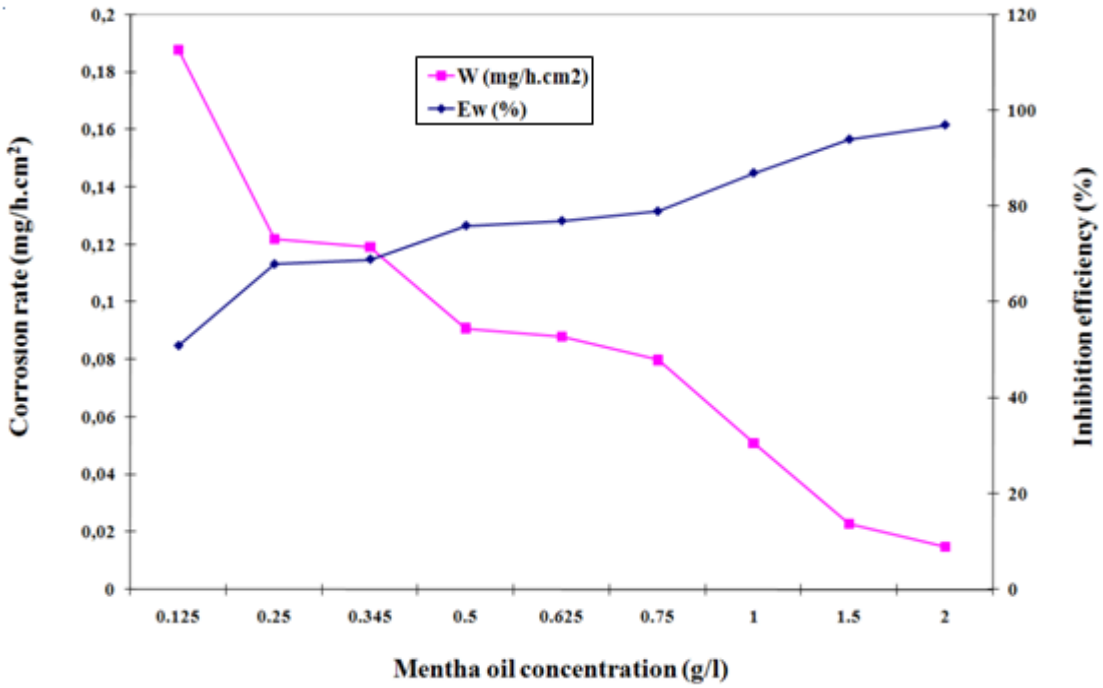

Figure 1. Variation of corrosion rate and inhibition efficiency of steel in 1M HCl without and with *M. Spicata* oil.

$$E_I\,\% = \frac{I_{corr} - I_{corr(inh)}}{I_{corr}} \times 100 \qquad (2)$$

where I_{corr} and $I_{corr\ (inh)}$ are the corrosion current density values without and with the inhibitor, respectively, determined by extrapolation of cathodic Tafel lines to the corrosion potential.

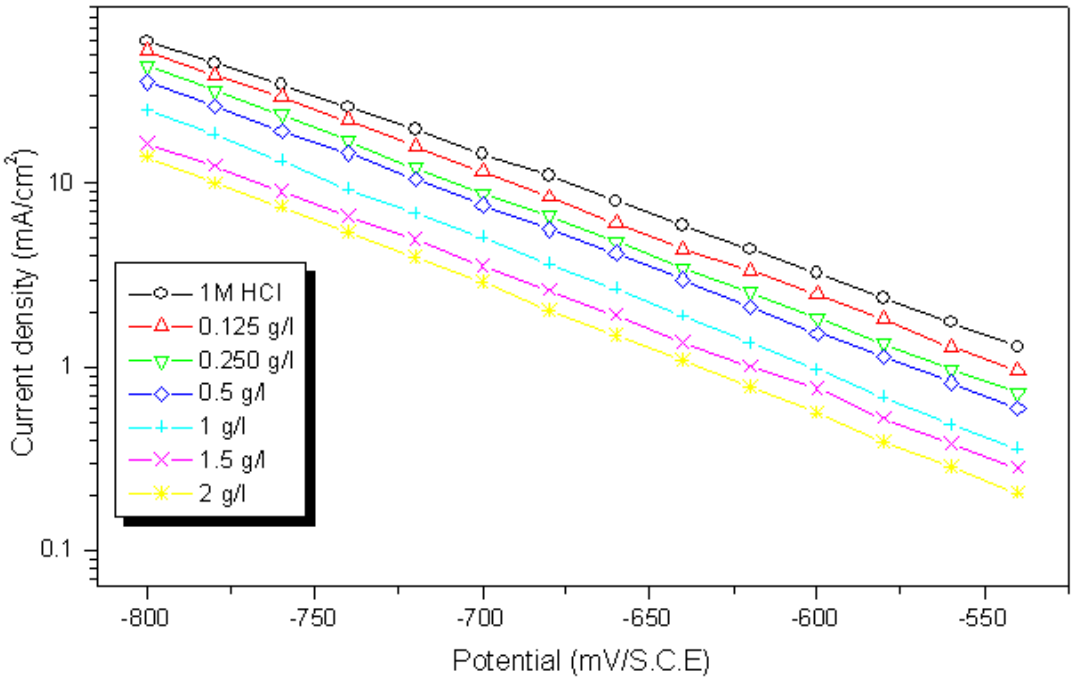

Figure 2. Cathodic plots of steel in 1M HCl at various concentrations of *Mentha* oil

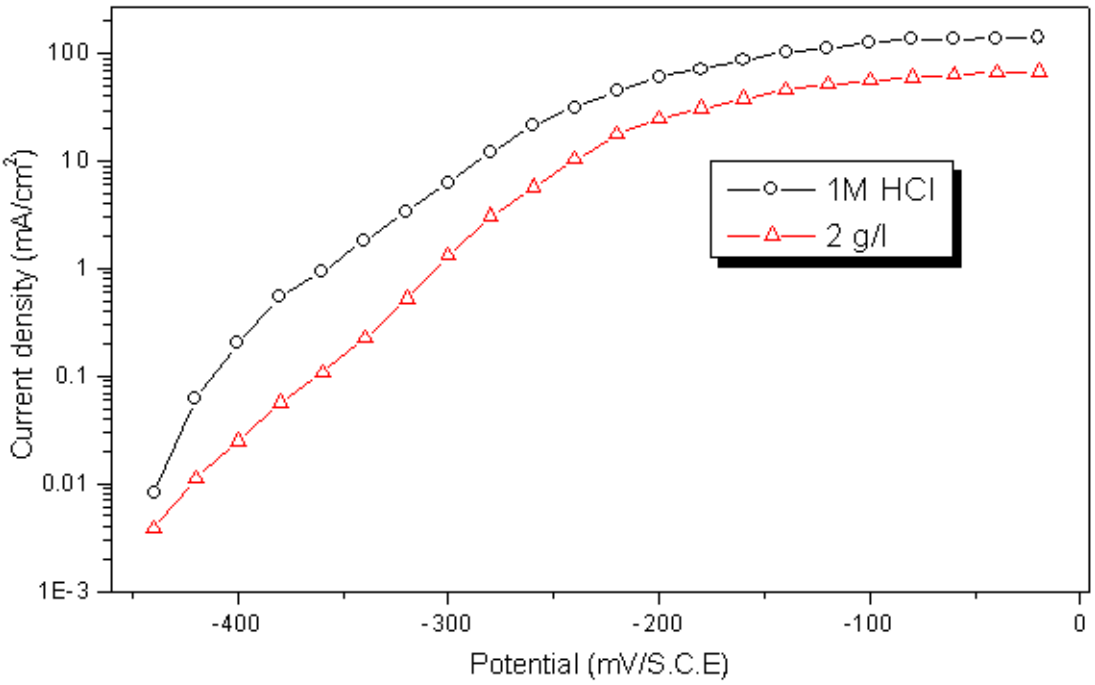

Figure 3. Anodic curves of steel in 1M HCl without and with *Mentha* oil.

Table 3. Electrochemical parameters of steel at various concentrations of *Mentha* oil studied in 1M HCl at 298 K. Corresponding corrosion inhibition efficiencies.

Inhibitor	Concentration (g/l)	E_{corr} (mV/SCE)	β_c (mV/dec)	I_{corr} ($\mu A/cm^2$)	E_I (%)	R_P ($\Omega.cm^2$)	E_{Rp} (%)
Blank	-	-396	176	78	-	68	-
Mentha oil	0.125	-398	175	40.5	48	136	50
	0.250	-400	172	27.3	65	200	66
	0.50	-402	172	19.5	75	272	75
	1.00	-397	174	14	82	358	81
	1.50	-400	178	10	87	567	88
	2.00	-395	175	5	94	971	93

The inhibiting properties of the tested Mentha oil have also been evaluated by the determination of the polarisation resistance. The corresponding polarisation resistance (R_P) values of steel in 1M HCl in the absence of different concentrations of the inhibitor are given in Table 2. The inhibition efficiency (E_{Rp}) was defined as follow:

$$E_{R_p}\% = \frac{R'_p - R_p}{R'_p} \times 100 \qquad (3)$$

R_P and R'_P are the polarisation resistance in the absence and in presence of the inhibitor, respectively.

From electrochemical polarisation measurements, it is clear from the results that the addition of inhibitor causes a decrease of the current density. The values I_{corr} of steel in the inhibited solution are smaller than those for the inhibitor free solution (Table 3). The parallel cathodic Tafel plots obtained in Fig. 2 indicate that the hydrogen evolution is activation-controlled and the reduction mechanism is not affected by the presence of inhibitor. The addition of inhibitor does not change the values of corrosion potential (E_{corr}) and cathodic Tafel slope (βc) when the concentration increases. These results demonstrate that the hydrogen evolution reaction is inhibited and that the inhibition efficiency increases with inhibitor concentration.

In the anodic range (Fig. 3), the polarisation curves of steel show that the addition of the natural oil decreases the current densities in large domain of potential. This result suggests that this compound act as a mixed-type inhibitor.

The corresponding polarisation resistance (R_p) values of steel in 1M HCl in the absence and presence of different concentrations of the tested inhibitor are also given in Table 2. We remark that R_p increases with increasing of inhibitor concentration to attain 93 % at 2.00 g/l. The inhibition efficiencies of inhibitor (natural oil) obtained by electrochemical methods are in good agreement.

3.4. Electrochemical impedance spectroscopy (EIS)

The corrosion behaviour of steel in 1M hydrochloric acidic solution, in the absence and presence of Mentha oil, is also investigated by the electrochemical impedance spectroscopy (EIS) at 298 ± 1 K after 30min of immersion. The charge-transfer resistance (R_t) values are calculated from the difference in impedance at lower and higher frequencies, as suggested by Tsuru and al. [21]. The double layer capacitance (C_{dl}) and the frequency at which the imaginary component of the impedance is maximal ($-Z_{max}$) are found as represented in equation:

$$C_{dl} = \frac{1}{\omega . R_t} \quad \text{where} \quad \omega = 2\,\pi\,.\,f_{max} \qquad (4)$$

Impedance diagrams are obtained for frequency range 100 KHz –10 mHz at the open circuit potential for steel in 1M HCl in the presence and absence of Mentha oil. Nyquist plots for steel in 1M HCl at various concentrations of Mentha oil are presented in Fig 4.

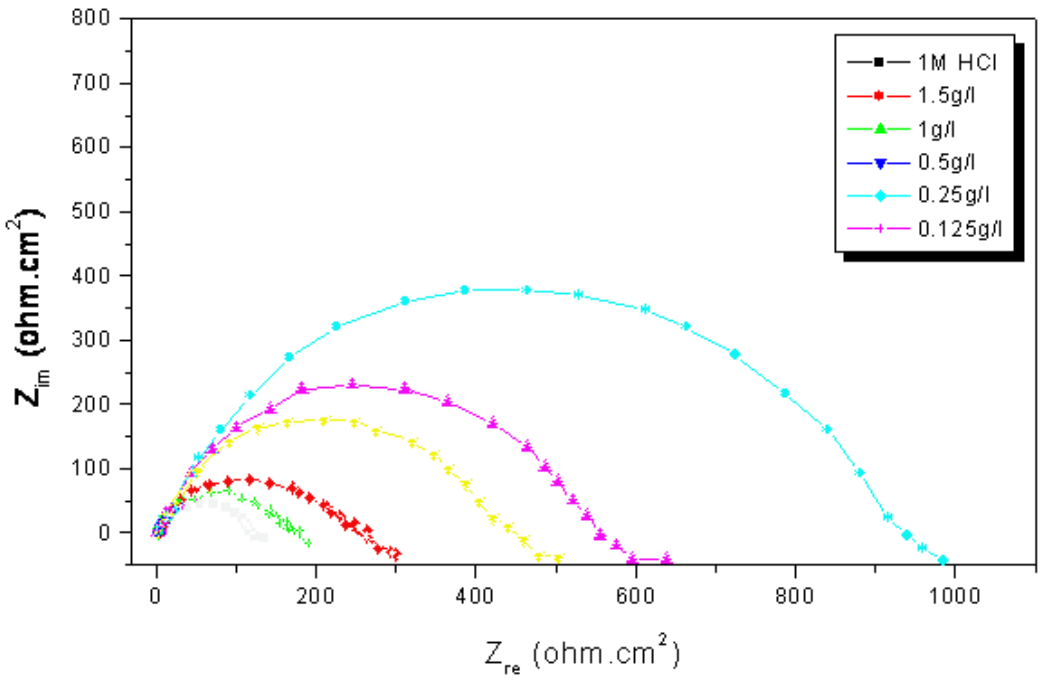

Figure 4. Nyquist plots of steel in 1M HCl containing various concentrations of *Mentha* oil.

Table 4 gives values of charge transfer resistance, R_t double-layer capacitance, C_{dl}, and f_{max} derived from Nyquist plots and inhibition efficiency, the inhibition efficiency got from the charge-transfer resistance is calculated by the following relation:

$$E_{Rt}\,\% = \frac{R'_t - R_t}{R'_t} \times 100 \qquad (5)$$

R_t and R'_t are the charge-transfer resistance values without and with inhibitor respectively. R_t is the diameter of the loop.

Table 4. Characteristic parameters evaluated from the impedance diagram for steel in 1M HCl at various concentrations of *Mentha* oil.

Inhibitor	Concentration (g/l)	R_t ($\Omega.cm^2$)	f_{max} (Hz)	C_{dl} ($\mu F/cm^2$)	E_{Rt} (%)
Blank	-	120	15.86	83.58	-
Mentha oil	0.125	240	18.00	73,65	50
	0.250	343	7.23	64,17	65
	0.50	500	5.41	58,77	76
	1	600	4.85	54,68	80
	1.5	1000	3.16	50.35	88

From the impedance data (Table 4), we conclude that the R_t values increase with inhibitor concentration and consequently the inhibition efficiency increases. As we notice, Fig. 4, the impedance diagrams consists of one large capacitive loop and they are not perfect semicircles and this difference has been attributed to frequency dispersion [22].

In fact, the presence of Mentha oil is accompanied by the increase of the value of R_t in acidic solution indicating a charge transfer process mainly controlling the corrosion of steel. Values of double layer capacitance are also brought down to the maximum extent in the presence of inhibitor and the decrease in the values of C_{dl} follows the order similar to that obtained for I_{corr} in this study. The decrease in C_{dl} is due to the adsorption of the inhibitor on the metal surface leading to the formation of film or complex from acidic solution [23].

3.5. Effect of temperature

The effect of temperature on the corrosion behaviour of steel in 1M HCl containing inhibitor at a concentration 2.00 g/l is studied in the temperature range 303-333K using weight loss measurements. Table 5 regroups the corresponding results obtained.

Table 5 Effect of temperature on the steel corrosion in the presence and absence of 2.00 g/l oil for 1 hour.

Temperature (K)	W' ($mg/cm^2.h$)	W ($mg/cm^2.h$)	E(%)
303	1,476	0,410	72
313	3,222	0,996	69
323	8,89	3,141	65
333	16,6	6,187	63

It is obvious that the corrosion rate increases both in the uninhibited and inhibited acid solution with the rise of temperature. The presence of inhibitor leads to decrease of the corrosion rate. E% depends upon the temperature and decreases with temperature.

The following relation can determine the apparent activation energy:

$$W_{corr} = k \exp(-E_a / RT) \text{ and } W'_{corr} = k' \exp(-E'_a / RT) \quad (6)$$

W'_{corr} and W_{corr} are the corrosion rates of steel with and without inhibitor, respectively. E_a' and E_a are the apparent activation energies in the presence and absence of inhibitor, respectively.

Arrhenius plots for the corrosion rates of steel are shown in Fig 5. The calculated values of activation energies from the slopes are 68,66 and 76,96 kJ/mol for free acid and with the addition 2.00 g/l of Mentha spicata oil, respectively.

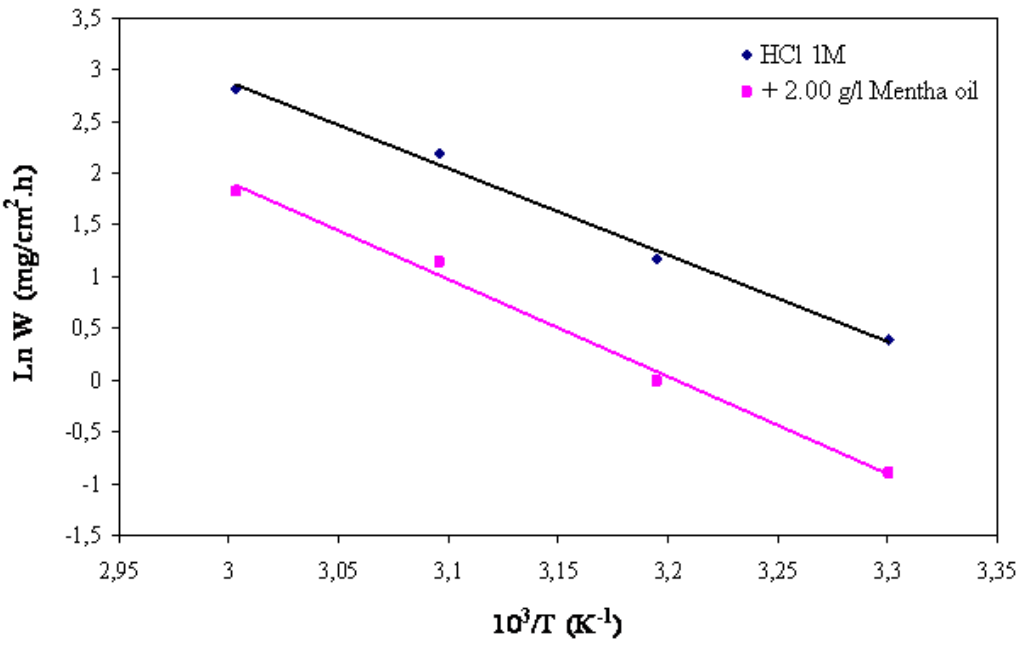

Figure 5. Arrhenius plots of steel in uninhibited and inhibited acid

3.6. Adsorption isotherm

It is found that the activation energy is increased in the presence of inhibitor. Furthermore, the decrease of E% is explained as physisorption of inhibitor molecule on the steel surface [24]. The lower value of E_a of the corrosion process in an inhibitors presence when compared to that in its absence is attributed to its chemisorption [25].

The dependence of the fraction of the surface covered Θ obtained by the ratio E%/100 as function of the oil concentration (C) was graphically fitted for Langmuir, Temkin and Frumkin adsorption isotherms. Fig 6 shows the dependence of C/Θ as function of the oil concentration. The

curve obtained clearly shows that the data fit well with Langmuir adsorption isotherm was found to be the best description of the adsorption behaviour of the studied inhibitor, which obeys:

$$\frac{C}{\theta} = \frac{1}{K_{ads}} + C \qquad (7)$$

C_{inh} is the inhibitor concentration; θ is the fraction of the surface covered, K_{ads} is the adsorption coefficient.

The literature shows that the adsorption of heterocyclic compounds occurs with the aromatic rings mostly perpendicular with respect of the metal surface at low concentration, but at elevated inhibitor concentration the molecules are reoriented to the parallel mod [26]. Besides, the adsorption phenomenon may be made by carvone as the principal constituent of the essential oil of Mentha spicata. But as the natural oil contains so many components, the inhibitory action may also due to synergistic intermolecular of the active molecules of this oil [24].

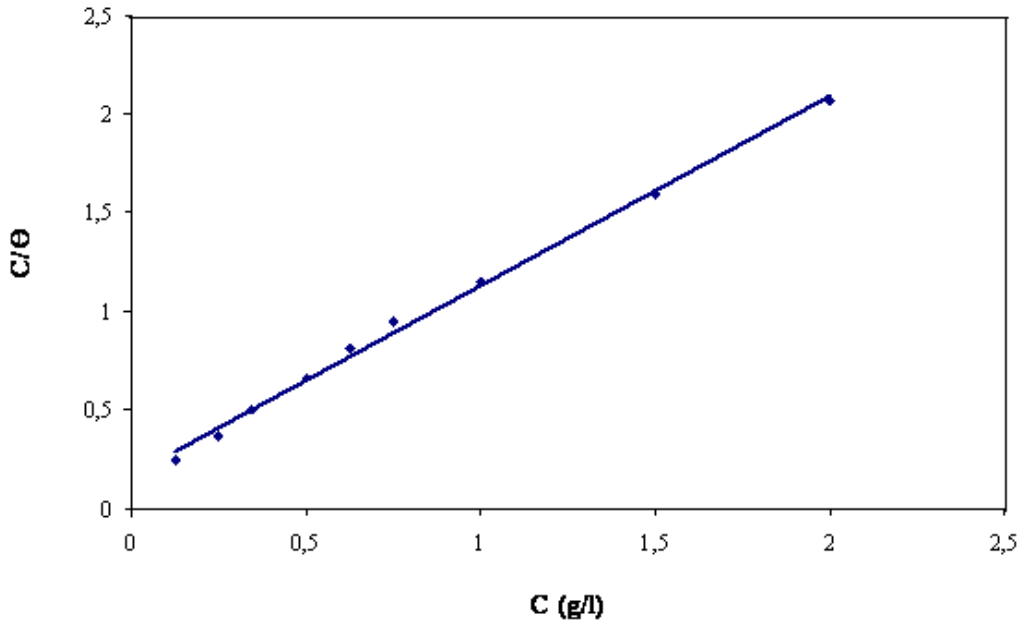

Figure 6. Langmuir adsorption isotherm of menthe oil on the steel surface

4. CONCLUSION

From the overall experimental results the following conclusions can be deduced:

- Chemical analysis showed carvone as major component of Mentha spicata L.,essential oil.
- *Mentha spicata* oil acts as good inhibitor for the corrosion of steel in HCl medium;

- The inhibition efficiency of *Mentha spicata* oil increases with concentration to attain 97% at 2.00 g/l;
- The inhibition efficiency of *Mentha spicata* oil decreases with the rise of temperature.
- The *Mentha* essential oil acts on steel surface as mixed inhibitor with a physisorption mechanism

References

1. A.Y. El-Etre, *Corros. Sci.* 45 (2003) 2485.
2. S. Martinez, I. Stern, *App. Surf. Sci*. 199 (2002) 83.
3. R.M. Saleh, A.A. Ismail, A.A. El Hosary, *Corros. Sci*. 17 (1982) 131.
4. A.A. El Hosary, R.M. Saleh, A.M. Shams El Din, *Corros. Sci*. 12 (1972) 897.
5. A. Bouyanzer, B. Hammouti, L. Majidi, *Material Letters*. 60 (2006) 2840.
6. A. Bouyanzer, L. Majidi, B. Hammouti, *Bull. Electrochem*. 22 (2006) 321.
7. A. Bouyanzer, B. Hammouti, L. Majidi, B. Haloui, *Portug. Electrochim. Acta* 28 (2010) 165.
8. Z. Faska, L. Majidi, R. Fihi, A. Bouyanzer, B. Hammouti, *Pigment & Resin Technol*. 36 (2007) 293.
9. O. Ouachikh, A. Bouyanzer, M. Bouklah, J-M. Desjobert, J. Costa. B. Hammouti, L. Majidi, *Surf. Rev. and Letters*. 16 (2009) 49.
10. H.J. Dorman, M. Kosar, K. Kahlos, Y. Holm, R. Hiltunen, *J. Agric. Food Chem.* 51 (2003) 4563.
11. S. Kokini, R. Karousou, L. Lenaras, *Biochem. Syst. Ecol*. 23 (1995) 425.
12. L. Jirovetz, G. Buchbauer, M. Shabi, M.B. Ngassoum, *Perfum. Flav*. 27 (2002) 16.
13. B.M. Lawrence, Mint: The Genus *Mentha*, CRC Press, Boca Raton, FL (2006).
14. J. F. Clevenger, *J. Am. Pharm. Assoc*. 17 (1928): 346.
15. National Institute of Standards and Technology. NIST WebBook (06/2005): http://webbook.nist.gov/ chemistry.
16. W.A. König, D.H. Hochmuth, D. Joulain, Terpenoids and Related Constituents of Essential Oils. Library of MassFinder 2.1, Institute of Organic Chemistry, Hamburg, Germany, 2001.
17. R.P. Adams, Identification of Essential Oil Components by Gaz Chromatography/Quadrupole Mass Spectroscopy. Allured Publishing: Carol Stream. 2001.
18. R.S. Chauhana, M.K. Kaula, A.K. Shahia, Arun Kumara, G. Rama, Aldo Tawa, *Industr. Crops and Prod*. 29 (2009) 654.
19. A.K. Shahi, S. Chandra, R. Gupta, M.K. Kaul, *Indian Perfum*. 5 (2007) 37.
20. A. Fahlen, M. Walander, R. Wennersten, *J. Sci. Food Agric*. 73 (1997) 111.
21. T. Tsuru, S. Haruyama, B. Gijutsu, *J. Jpn. Soc. Corros. Eng*. 27 (1978) 573.
22. F. Mansfeld, M.W. Kending, *S. Tsai, Corrosion*. 37 (1981) 301; ibid 38 (1982) 570.
23. F. Bentiss, M. Lagrenée, M. Traisnel, J.C. Hornez, *Corros. Sci*. 41 (1999) 789.
24. M. Dahmani, A. Et-Touhami, S.S. Al-Deyab , B. Hammouti, A. Bouyanzer, *Int. J. Electrochem. Sci.*, 5 (2010) 1060.
25. A. Zarrouk, I. Warad, B. Hammouti, A Dafali, S.S. Al-Deyab, N. Benchat, *Int. J. Electrochem. Sci.*, 5 (2010) 1516.
26. J.O.M. Bockris, B. Young, *J. Electrochem. Soc*. 138 (1999) 2237.